The tumor suppressor DAPK inhibits cell motility by blocking the integrin-mediated polarity pathway

Jean-Cheng Kuo,[1] Won-Jing Wang,[1] Chung-Chen Yao,[2,3] Pei-Rung Wu,[1] and Ruey-Hwa Chen[1]

[1]Institute of Molecular Medicine and [2]Department of Orthodontics, College of Medicine, and [3]Department of Dentistry, National Taiwan University Hospital, National Taiwan University, Taipei 106, Taiwan

Death-associated protein kinase (DAPK) is a calmodulin-regulated serine/threonine kinase and possesses apoptotic and tumor-suppressive functions. However, it is unclear whether DAPK elicits apoptosis-independent activity to suppress tumor progression. We show that DAPK inhibits random migration by reducing directional persistence and directed migration by blocking cell polarization. These effects are mainly mediated by an inhibitory role of DAPK in talin head domain association with integrin, thereby suppressing the integrin–Cdc42 polarity pathway. We present evidence indicating that the antimigratory effect of DAPK represents a mechanism through which DAPK suppresses tumors. First, DAPK can block migration and invasion in certain tumor cells that are resistant to DAPK-induced apoptosis. Second, using an adenocarcinoma cell line and its highly invasive derivative, we demonstrate DAPK level as a determining factor in tumor invasiveness. Collectively, our study identifies a novel function of DAPK in regulating cell polarity during migration, which may act together with its apoptotic function to suppress tumor progression.

Introduction

Cell migration is crucial for many biological processes, including embryonic development, wound healing, and immune surveillance. Migration is a complex and highly coordinated process that requires a cell to polarize, extend protrusions in the direction of movement, form adhesions at the leading edge, translocate the cell body, and, finally, detach from the substratum at the trailing edge (Lauffenburger and Horwitz, 1996; Ridley et al., 2003). Directed cell migration is usually initiated in response to extracellular cues such as chemoattractants, growth factors, and the extracellular matrix. The establishment and maintenance of polarity during directed migration are mediated by feedback regulations involving integrins, phosphoinositides, cytoplasmic adaptor proteins, and Rho family guanosine triphosphatases (GTPases; Ridley et al., 2003).

The Rho family GTPase Cdc42 plays a crucial role in determining cell polarity during directed migration. Cdc42 is activated at the leading edge of polarized cells (Itoh et al., 2002) and inhibition of Cdc42 activity or expression impairs directed migration assayed either in the cell culture system (Allen et al., 1998; Nobes and Hall, 1999) or in vivo (Stramer et al., 2005). Studies on slow moving cells such as astrocytes and fibroblasts indicate that Cdc42 controls polarized migration through two mechanisms. First, Cdc42 restricts the formation of protrusions at the front, which is mediated by a spatially specific activation of Rac at the leading edge, thereby promoting a polarized actin polymerization activity toward the direction of migration (Cau and Hall, 2005). Second, Cdc42 is required for the reorientation of the microtubule-organizing center (MTOC) and Golgi to face the direction of migration (Nobes and Hall, 1999; Etienne-Manneville and Hall, 2001), which may contribute to polarity establishment by facilitating microtubule growth to the lamella and directed vesicle transport to the leading edge to maintain forward protrusions (Raftopoulou and Hall, 2004). The effect of Cdc42 on MTOC and Golgi positioning is mediated through the Par6–Par3–aPKC complex (Etienne-Manneville and Hall, 2001), which inactivates glycogen synthase kinase-3β to promote the capture of microtubule plus ends at the leading edge via adenomatosis polyposis coli (Etienne-Manneville and Hall, 2003). Another mediator of Cdc42-induced MTOC polarization is IQGAP1, which forms a complex with two microtubule plus end–binding proteins, CLIP-170 (Fukata et al., 2002) and adenomatosis polyposis coli (Watanabe et al., 2004). Together, these findings indicate that Cdc42 coordinately regulates both actin and microtubule cytoskeletons via distinct pathways, thereby establishing the polarized morphology.

Correspondence to Ruey-Hwa Chen: rhchen@ha.mc.ntu.edu.tw

Abbreviations used in this paper: DAPK, Death-associated protein kinase; MLC, myosin light chain; MTOC, microtubule-organizing center; pFAK, phosphorylated FAK; siRNA, small interfering RNA; talin-H, talin head domain.

The online version of this article contains supplemental material.

The Journal of Cell Biology, Vol. 172, No. 4, February 13, 2006 619–631
http://www.jcb.org/cgi/doi/10.1083/jcb.200505138

It has been implicated that integrins act upstream of Cdc42 during directed migration. Although the function of integrin in migration is best known to be involved in the formation of cell adhesions, emerging evidence has revealed its role in cell polarization. For instance, integrin α5β1 mediates fibronectin-dependent cell polarization and protrusion through Rho family GTPases (Cox et al., 2001). Integrin engagement is also essential for Cdc42 activation and polarity establishment during wound-healing migration (Etienne-Manneville and Hall, 2001). Recently, α4 integrin was found to regulate cell polarity by recruiting the paxillin–GIT1 complex, in which GIT1 functions as an Arf-GAP to decrease Arf6 activity, thereby leading to Rac inhibition. As this complex is spatially restricted to the sides and the rear of the cell, Rac activation is limited to the leading edge, thus facilitating directed migration (Nishiya et al., 2005). Despite these findings, it remains unclear whether proteins that affect integrin activity could influence cell polarity during migration.

Death-associated protein kinase (DAPK) is a calmodulin-regulated and cytoskeleton-associated serine/threonine kinase (Deiss et al., 1995). Several lines of evidence indicate that DAPK plays an important role in tumor suppression. First, the expression of DAPK is frequently lost in various human cancer cell lines and tumor tissues, and this loss of expression correlates strongly with the recurrence and/or metastasis incidence of several human cancers (for reviews see Raveh and Kimchi, 2001; Bialik and Kimchi, 2004). Second, the antitumorigenic effect of DAPK was directly demonstrated in a mouse model system in which DAPK expression plays a causative role in suppressing the ability of Lewis lung carcinoma to form metastases in mice (Inbal et al., 1997). Third, DAPK is capable of suppressing c-myc– and E2F-induced oncogenic transformation by activating a p53-mediated apoptotic pathway (Raveh et al., 2001).

The tumor-suppressive function of DAPK has been attributed to its effect on promoting apoptosis. DAPK is a well known proapoptotic protein and participates in a wide variety of apoptotic paradigms (Deiss et al., 1995; Cohen et al., 1997, 1999; Inbal et al., 1997; Raveh et al., 2001; Jang et al., 2002; Pelled et al., 2002; Yamamoto et al., 2002). Recently, we found that DAPK exerts an apoptotic effect by inside-out inactivation of integrin β1, thereby suppressing the matrix survival signal and activating a p53-dependent apoptosis pathway (Wang et al., 2002). Accordingly, the proapoptotic activity of DAPK is largely dependent on the existence of functional p53 protein, and several p53-deficient cell lines either escape from cell death (Wang et al., 2002) or undergo autophagic death in response to DAPK overexpression (Inbal et al., 2002). However, given the broad involvement of DAPK in tumor suppression and the frequent loss or mutation of p53 in various tumors, we postulate that DAPK elicits the second, apoptosis-unrelated mechanism to suppress tumor progression. Notably, the effects of DAPK on integrin inactivation (Wang et al., 2002) and actin cytoskeleton reorganization (Kuo et al., 2003; Bialik et al., 2004) raise the possibility of DAPK involvement in motility regulation.

We demonstrated that DAPK interferes with directional persistence during random migration and with cell polarization during directed migration and that these effects of DAPK are mainly mediated by its suppression of the integrin–Cdc42 signaling axis. Even in tumor cells that are resistant to DAPK-induced apoptosis, DAPK can elicit this motility-inhibitory effect and functions as a determining factor in tumor cell invasion. Together, our study identifies a novel role of DAPK in regulating cell polarity during migration, which may contribute in part to the tumor-suppressive function of DAPK.

Results

DAPK inhibits random migration by reducing directional persistence

To characterize the function of DAPK in cell motility, we first examined whether DAPK affects the migration of free-moving fibroblasts. NIH3T3 cells were infected with retrovirus carrying control vector, DAPK, DAPK42A (a dominant-negative mutant), or DAPKΔCaM (a constitutively active mutant; Cohen et al., 1997), together with a puromycin-resistant gene. After selection with puromycin, pools of cells that overexpressed various DAPK proteins were generated (Fig. 1 A). Because prolonged culture of cells overexpressing DAPK or DAPKΔCaM led to apoptosis (Wang et al., 2002), populations of cells were used immediately after selection to test for their migration using time-lapse microscopy. We first observed that the four populations of cells exhibited different morphologies. Cells expressing DAPK or DAPKΔCaM often displayed many protrusions all around the cells, and these protrusions extended and retracted frequently during cell migration (Fig. 1 B and Video 1, available at http://www.jcb.org/cgi/content/full/jcb.200505138/DC1). Cells carrying control vector or DAPK42A, however, often showed a long and polarized morphology (Fig. 1 B) and, consequently, less protrusions (Fig. 1 C) and smaller spreading areas (Fig. 1 D) than the other two populations. When analyzing the trajectory of each individual cell during a 120-min migration period by tracing its centroid from the time-lapse movie, we found that cells expressing DAPK or DAPKΔCaM displayed much shorter net translocation than the control cells, whereas cells expressing DAPK42A showed longer paths (Fig. 1 B, right). Furthermore, the DAPK- or DAPKΔCaM-expressing cells made directional changes much more frequently than cells carrying control vector, whereas the DAPK42A-expressing cells migrated on a straighter path. These effects on random migration could be more clearly visualized by reproducing sample cell movement paths on window plots (Fig. 1 E). Fig. 1 F showed the rates of cell migration, the distances of net translocation during the 120-min time period, and the directional persistence of cells. These analyses revealed that each type of cell did not display a significant difference in their migration rate and that the differences in their net translocation were mainly attributed to their directional persistence properties during migration. Together, our data indicate that DAPK inhibits random migration by reducing the directional persistence.

DAPK inhibits directed migration by interfering with cell polarization

The reduced directional persistence suggests that DAPK renders cells unable to maintain a stable direction during targeted migration. Therefore, we assayed these NIH3T3 derivatives for wound-healing migration. Similar to what was observed with free-moving

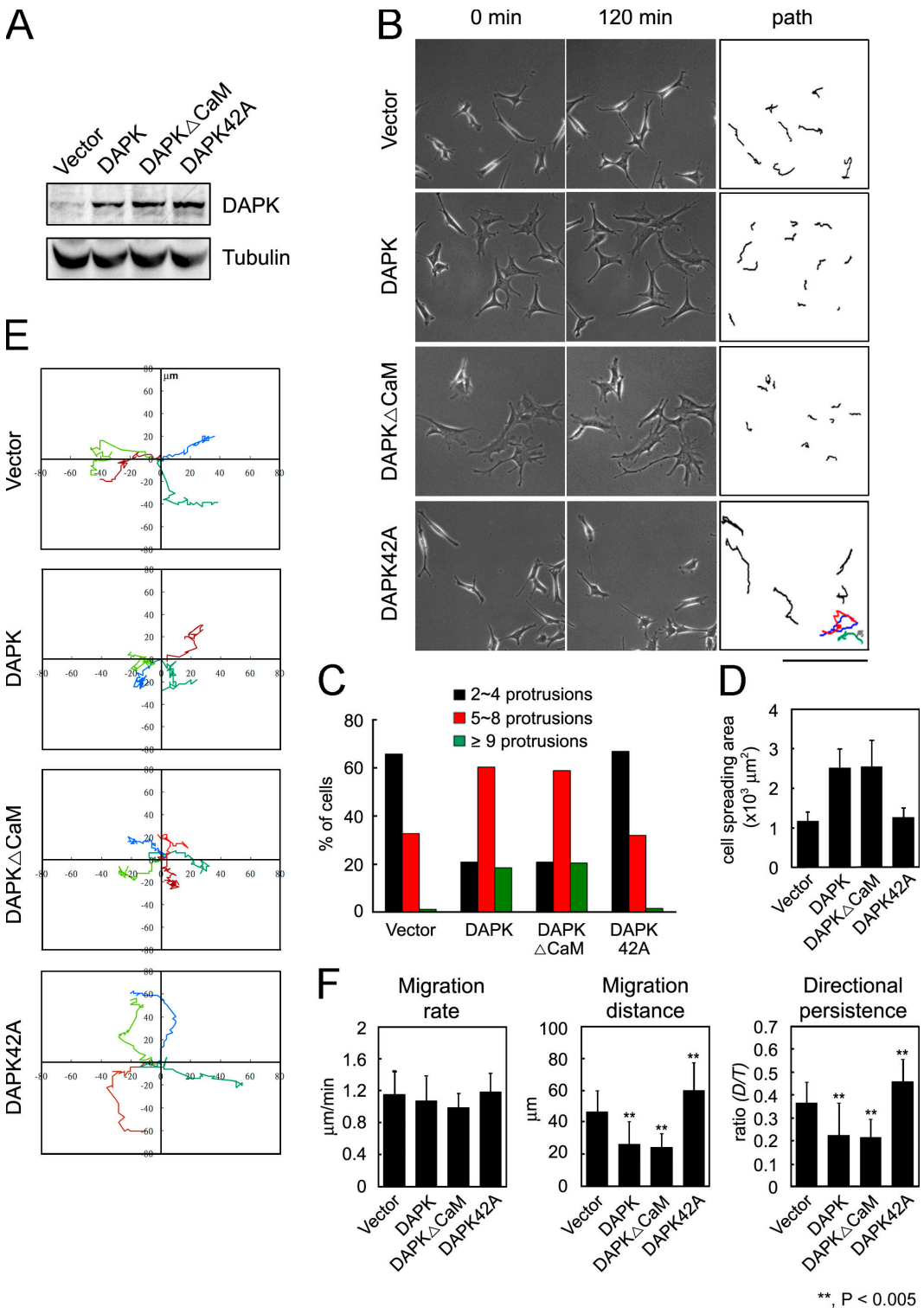

Figure 1. **Effects of DAPK on random migration.** (A) NIH3T3 cells were infected with recombinant retrovirus carrying vector or various forms of DAPK, selected by puromycin, and subjected to immunoblot analyses with antibodies as indicated. (B) Morphologies and migratory behaviors of NIH3T3 cells expressing various DAPK proteins. Cells as in A were plated and monitored 30 h after plating. (left and middle) Images at 0 and 120 min, respectively. (right) These images delineate the path of each cell during the 120-min period. Colored lines are used to distinguish overlapped cell paths. Video 1 corresponds to this figure. (C) Regulation of cell protrusions by DAPK. Protrusions longer than 5 μm formed per cell were quantitated based on time-lapse images. The percentage of cells in each population having protrusions within the indicated ranges was calculated and plotted. For each cell population, at least 300 cells were scored. (D) Areas of spreading were measured using Metamorph software and plotted. Data shown are means ± SD. $n = 50$. (E) Analysis of migration paths. The tracks of representative cells shown in B were plotted. The origins of migration were superimposed at 0, 0. (F) Migration parameters were calculated as described in Materials and methods. Data represent means ± SD from trajectories of 30 cells. **, $P < 0.005$, as compared with cells with control vector. Video 1 is available at http://www.jcb.org/cgi/content/full/jcb.200505138/DC1. Bar, 200 μm.

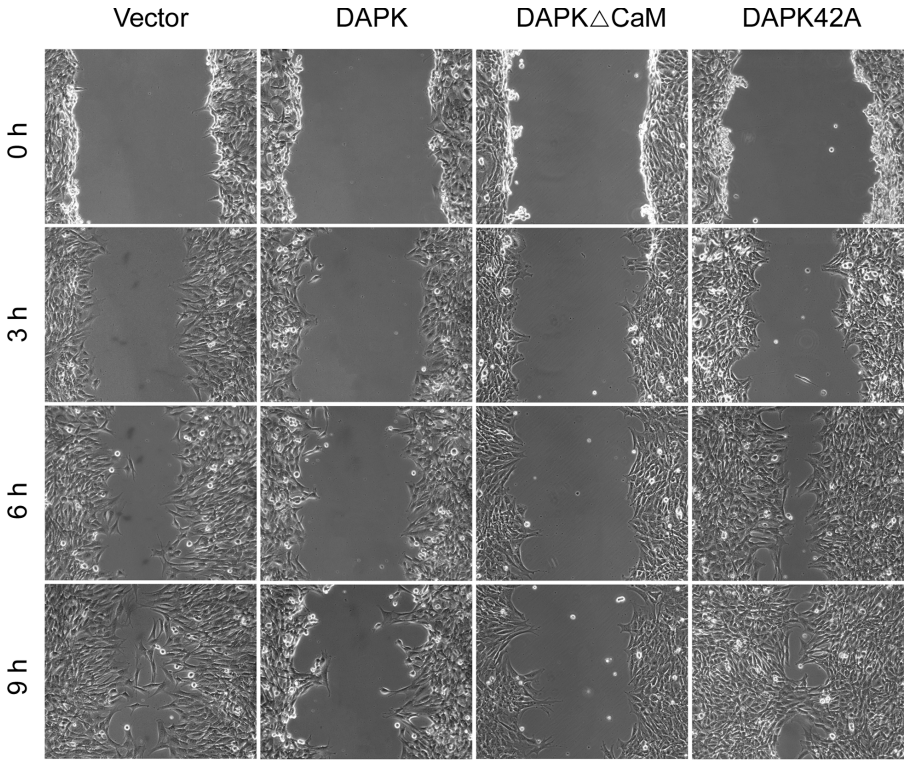

Figure 2. **Effect of DAPK on wound-healing migration.** Cells, as in Fig. 1, were assayed for wound-healing migration, and cell migration into wounds was monitored by time-lapse microscopy. Still images were captured at the indicated times after wounding. Bar, 200 μm.

cells, overexpression of DAPK or DAPK ΔCaM caused a marked delay in wound closure, whereas DAPK42A accelerated wound closure (Fig. 2). Close examination of cells at the wound edge revealed that control cells displayed a polarized phenotype, with cell protrusions perpendicular to the wound and microtubules elongating to the tip of protrusions (Fig. 3, A and B; and Video 2, available at http://www.jcb.org/cgi/content/full/jcb.200505138/DC1). This polarization of wound-edge cells was also made evident by the reorientation of their MTOC and Golgi in the direction of wound (Fig. 3 B). Although the polarized phenotype was preserved in cells expressing DAPK42A, cells expressing DAPK or DAPKΔCaM manifested a drastic disruption of polarity. Although these cells still formed protrusions at the wound edge, their directions were more random, and a substantial proportion of cells displayed multiple short protrusions or protrusions parallel to the wound (Fig. 3 A and Videos 3–5, available at http://www.jcb.org/cgi/content/full/jcb.200505138/DC1). Furthermore, their microtubules showed scattered distribution, and a significantly lower number of cells in the front row exhibited polarized MTOC and Golgi (Fig. 3 B). Time course analysis indicated that the DAPK-expressing cells exhibited a delayed kinetics of Golgi reorientation compared with control cells, whereas DAPKΔCaM-expressing cells did not show reorientation, even 7 h after wounding. In contrast, cells expressing DAPK42A modestly accelerated wound-induced Golgi reorientation (Fig. 3 C). These observations collectively identify an inhibitory role of DAPK in cell polarization during directed migration.

DAPK blocks Cdc42 activation in response to migratory cues

Cdc42 activity is required for establishing polarity during directed migration (Nobes and Hall, 1999). To study the molecular mechanism through which DAPK inhibits the polarization of cells at the wound edge, we assessed the activity of Cdc42 during wound-healing migration. In cells carrying vector or DAPK42A, Cdc42 activity was drastically induced 15 min after wounding and then declined gradually. However, this wound-induced Cdc42 activation was delayed and modestly attenuated in DAPK-expressing cells and completely abrogated in DAPKΔCaM-expressing cells (Fig. 4, A and B). Therefore, we investigated whether the suppression of Cdc42 activation accounts for the polarity defects induced by DAPK. Indeed, expression of a constitutively active Cdc42 mutant rescued the Golgi polarization defect seen in DAPKΔCaM-expressing cells (Fig. 4, C and D). Thus, DAPK inhibits cell polarity by suppressing Cdc42 activation.

DAPK blocks integrin β1 activation at the leading edge of migrating cells

The migration-induced Cdc42 activation and cell polarization can be abolished by a cyclic RGD peptide, demonstrating a role for integrin in the establishment of cell polarity (Etienne-Manneville and Hall, 2001). Accordingly, we observed that integrin β1 was preferentially activated at the leading edge of migrating cells, as judged by comparing the distribution of total integrin β1 with that of activated β1 (Fig. 5 A). Intriguingly, DAPK was also localized at the leading edge of cells undergoing wound-healing migration (Fig. 5 A). Consistent with this DAPK distribution and a previously reported effect of DAPK on integrin inactivation (Wang et al., 2002), overexpression of DAPK or DAPKΔCaM attenuated integrin downstream signaling at the leading edge, as monitored by autophosphorylation of FAK (Fig. 5 B). FAK autophosphorylation at the leading edge was rescued by pretreatment of DAPK- or DAPKΔCaM-expressing

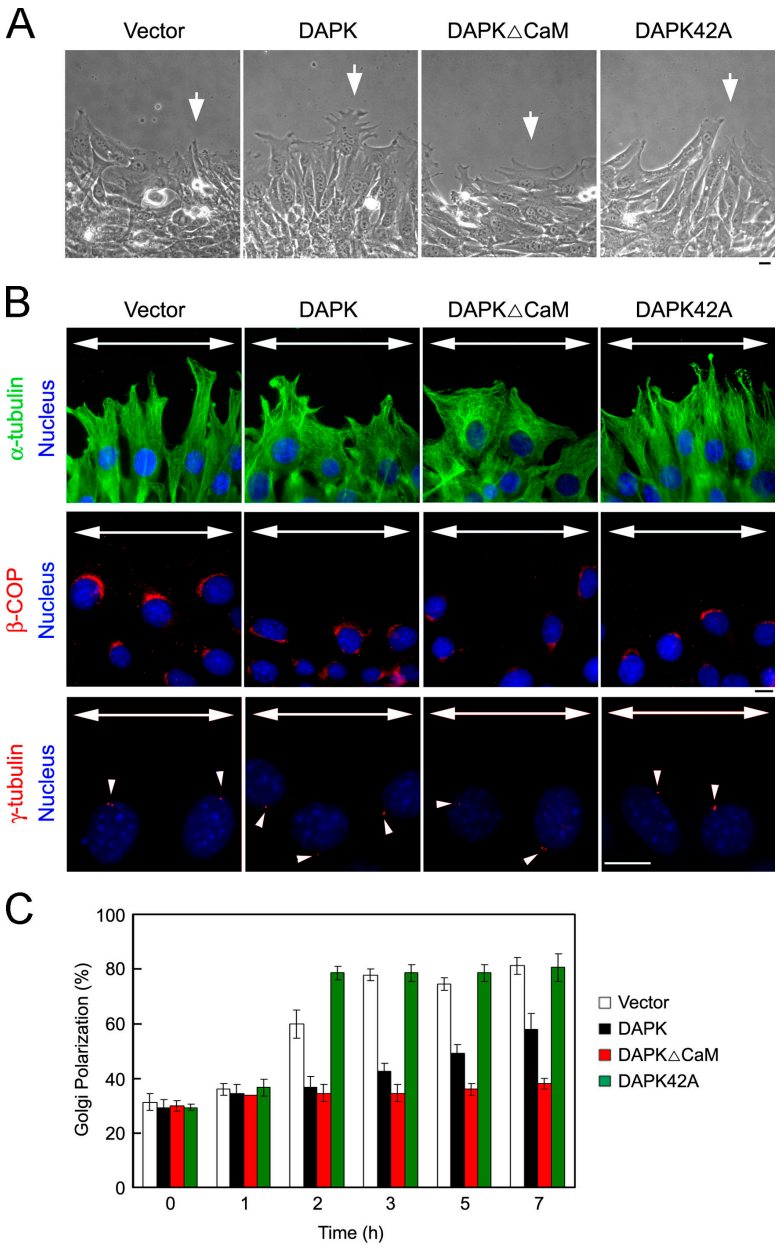

Figure 3. **DAPK interferes with cell polarization during wound-healing migration.** (A) The morphologies of wound-edge cells. A confluent monolayer of cells, as in Fig. 2, was wounded, and still images were taken 5 h after wounding. Arrows indicate the morphological differences of each population of cells at the wound edge. Videos 2–5 correspond to these images. (B) The effects of DAPK on microtubule polarization and Golgi and MTOC reorientation. Cells as in A were wounded and fixed at 5 h after wounding. Cells were double stained with Hoechst 33342 and anti–α-tubulin (to visualize microtubules), anti–β-COP (to visualize Golgi), or anti–γ-tubulin antibody (to visualize MTOC) and examined by fluorescence microscopy. Arrows indicate the direction of the wound, and arrowheads mark the locations of MTOC. (C) Kinetics of Golgi reorientation. The percentage of wound-edge cells with their Golgi apparatus in the forward-facing 120° sector was measured at the indicated time points after wounding. For each time point and cell population, at least 150 cells were scored. Data represent means ± SD. $n = 3$. Videos 2–5 are available at http://ww.jcb.org/cgi/content/full/jcb.200505138/DC1. Bars, 10 μm.

cells with the integrin β1–activating antibody TS2/16 (Fig. 5 B). Thus, these findings not only suggest the existence of polarized integrin β1 activity and signaling in cells at the wound edge, but also reveal an inhibitory role of DAPK in these polarized events.

DAPK signaling interferes with talin head domain (talin-H) binding to integrin β1 tail

Next, we explored the mechanism by which DAPK inactivates integrin. Integrin activation can be regulated by several Ras family GTPases, such as R-Ras and Rap1, and, at least in certain circumstances, R-Ras acts upstream of Rap1 for integrin activation (Kinbara et al., 2003). However, expression of DAPK or its mutants did not affect Rap1 activity, as monitored by a pull-down analysis (Fig. S1, available at http://www.jcb.org/cgi/content/full/jcb.200505138/DC1). Another important intracellular molecule for integrin activation is talin, which was recently found to be a common downstream effector of many signaling pathways that control integrin activation (Tadokoro et al., 2003). To investigate the role of talin in DAPK-triggered integrin inactivation, we used RNA interference to knockdown talin expression. The introduction of talin small interfering RNAs (siRNAs) to 293T cells led to a great reduction of talin expression, but not of cell surface expression of integrin β1, which was monitored by the β1-specific antibody AIIB2 (Fig. 6 A). As expected, this down-regulation of talin in 293T cells decreased the activity of integrin β1, as monitored by the monoclonal antibody B44, which specifically recognizes the active integrin β1 (Ni et al., 1998). A similar reduction of B44 binding was observed in cells overexpressing DAPK or DAPKΔCaM, which is consistent with our previous study (Wang et al., 2002). Conversely, DAPK42A led to an increase of

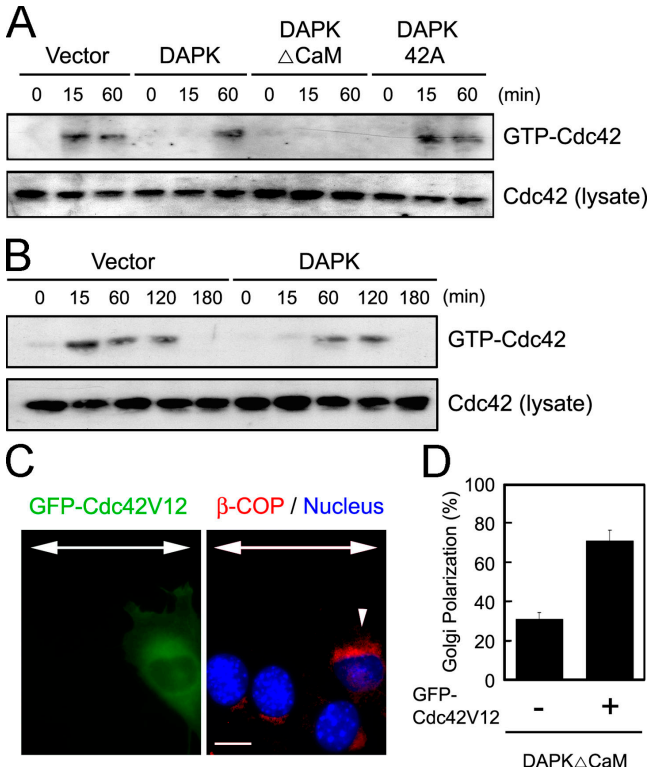

Figure 4. **DAPK disrupts cell polarity by blocking Cdc42 activation.** (A and B) NIH3T3 cells expressing various DAPK proteins were wounded as described in Materials and methods and lysed at indicated time points after wounding. (top) The amount of GTP-bound Cdc42 was determined by GST-PAK-CRIB pull-down analysis, followed by Western blotting with anti-Cdc42 antibody. (bottom) The levels of total Cdc42. (C) NIH3T3 cells expressing DAPKΔCaM were transiently transfected with pGFP-C1-Cdc42V12 and assayed for wound-healing migration. Cells were fixed 5 h after wounding and stained with anti–β-COP antibody and Hoechst 33342. Arrows indicate the direction of the wound, and the arrowhead marks the GFP-positive cell (right). (D) The percentage of GFP-positive and -negative cells, as in C, with polarized Golgi was measured in the front row cells. For each population, at least 150 cells were scored. Data represent means ± SD. $n = 3$. Bar, 10 μm.

B44 binding. However, in talin knockdown cells, the expression of DAPK or DAPKΔCaM could not further decrease the binding of B44, whereas DAPK42A could no longer increase B44 binding. Furthermore, activation of integrin by treatment of cells with Mn^{2+} completely rescued the effect of talin knockdown on DAPK42A-expressing cells (Fig. 6 B). Collectively, these results indicate that DAPK acts upstream of talin to inhibit its integrin activation function. We next tested whether DAPK elicits an inhibitory effect on the association of talin-H with integrin β1 tail. To avoid the detection of association induced by any post-adhesion event, we prepared lysate from suspension cells. We found that in suspension cells, the expression of DAPK or DAPKΔCaM reduced the capability of coexpressed talin-H to interact with bacterially expressed GST-β1 tail. Conversely, DAPK42A enhanced this association (Fig. 6 C). To investigate whether DAPK acts directly on talin-H to prevent its interaction with integrin β1 tail, we tested the possibility of talin-H as a DAPK substrate. In vitro kinase assay revealed that DAPK did not phosphorylate talin-H, whereas myosin light chain was heavily phosphorylated by DAPK (Fig. 6 D). Thus, DAPK may use an indirect mechanism to interfere with the recruitment of talin-H to integrin β1 tail. Nevertheless, as this DAPK-induced blockage of talin-H–integrin interaction could be detected in the absence of cell adhesion, this effect likely contributes to a mechanism by which DAPK inactivates integrin.

Enforced activation of integrin β1 rescues the migration defects of DAPK

We reasoned that the DAPK-induced inhibition of integrin may represent a mechanism by which DAPK suppresses wound-healing and random migrations. Indeed, enforced activation of integrin β1 by the mouse β1–activating antibody 9EG7 rescued wound-induced Cdc42 activation in NIH3T3 cells expressing DAPK or DAPKΔCaM (Fig. 7 A). Consequently, 9EG7 restored Golgi polarization (Fig. 7, B and C) and rescued wound-healing migration defects (Fig. 7 D) in these two populations of cells. Furthermore, in random migration, 9EG7 completely reversed the DAPK-induced defects in net cell translocation and directional persistence, and the four populations of cells moved in a similar manner under 9EG7 treatment (Fig. 7, E and F; and Fig. S2, available at http://www.jcb.org/cgi/content/full/jcb.200505138/DC1). Notably, integrin activation converted the morphology of DAPK- and DAPKΔCaM-expressing cells to a typical polarized morphology, i.e., with a single, stable protrusion at the leading edge and a long trailing tail (Video 6). As a control, a nonactivating integrin β1 antibody MB1.2 could not rescue the random migration defects induced by DAPK or DAPKΔCaM (Fig. 7 F). Thus, we conclude that inactivation of β1 integrin accounts for a major mechanism through which DAPK suppresses cell motility and migratory polarity.

DAPK suppresses migration and invasion of tumor cells that are resistant to its proapoptotic effect

Having demonstrated that DAPK effects motility inhibition in fibroblasts, we next investigated whether this function of DAPK could be recaptured in carcinoma cells that are resistant to the apoptotic effect of DAPK. As the proapoptotic activity of DAPK is largely dependent on the existence of functional p53 protein (Inbal et al., 2002; Wang et al., 2002), we used two human tumor cell lines that contain mutant p53, i.e., the epidermoid carcinoma cell A431 (Logunov et al., 2004) and the breast carcinoma cell MDA-MB-231 (Im et al., 2001). Again, DAPK or its mutants were introduced to the two cell lines by retrovirus-mediated gene transfer. Overexpression of DAPK or DAPKΔCaM in either cell line could not trigger apoptosis (Fig. S3 A, available at http://www.jcb.org/cgi/content/full/jcb.200505138/DC1). In fact, even maintained in culture for 26 d, these cells were still alive and expressed exogenous DAPK proteins at similar levels as those cultured for only 3 d (Fig. 8 A). When the four populations of A431 cells were assayed for wound-healing migration, we observed a substantial delay of wound closure in cells expressing DAPK or DAPKΔCaM, which was reversed by pretreatment of cells with TS2/16. In contrast, DAPK42A accelerated wound closure (Fig. 8 B and Fig. S3 B). The migratory capabilities of these stable lines were also tested with haptotactic migration assays. Similar to what was found in wound-healing

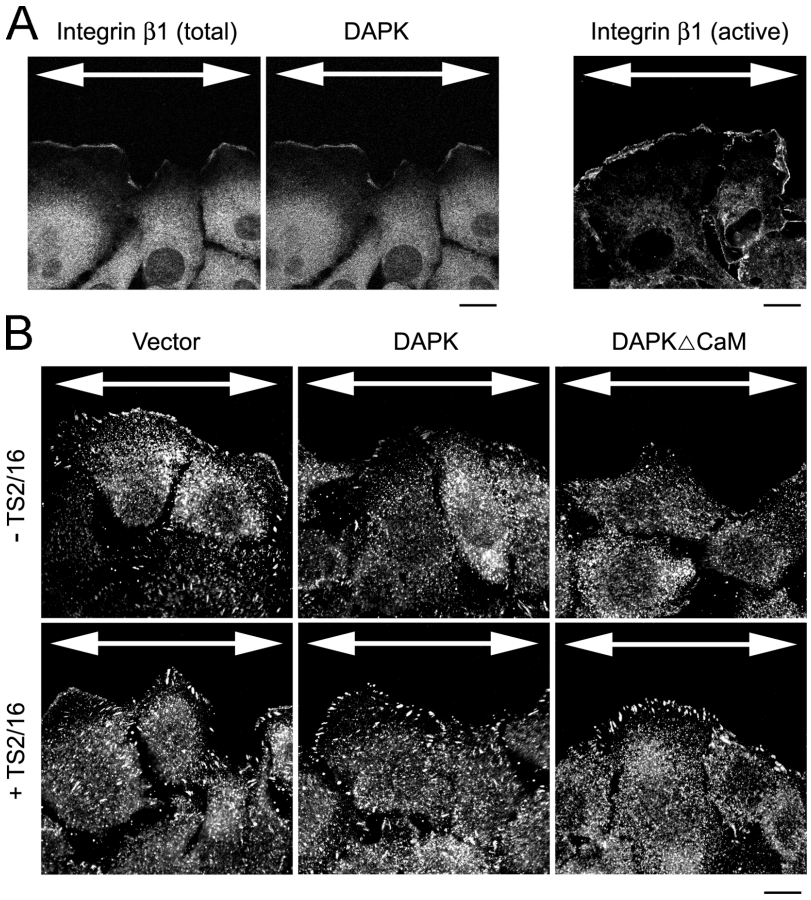

Figure 5. **Both wound-induced activation of integrin β1 and DAPK-induced blockage of integrin signaling occur at the leading edge.** (A) Activation of integrin β1 at the leading edge of a migrating cell. A monolayer of MDA-MB-231 cells was scratched and fixed 5 h later. Cells were double stained for total integrin β1 (with antibody P4C10) and DAPK or stained for active integrin β1 (with antibody B44) and examined by confocal microscopy. (B) DAPK blocks wound-induced FAK activation at the leading edge. MDA-MB-231 cells stably expressing various DAPK proteins (Fig. 8 A) were treated with or without TS2/16 before wounding and fixed 5 h later. Cells were stained with p-FAK and examined by confocal microcopy. Arrows indicate the direction of the wound. Bars, 10 μm.

migration, expression of DAPK or DAPKΔCaM greatly suppressed collagen-induced haptotactic migration of A431 cells, whereas DAPK42A promoted haptotaxis. Again, the effect of DAPK or DAPKΔCaM on haptotactic migration was completely overridden by TS2/16 (Fig. 8 C). Furthermore, we observed a similar inhibitory effect of DAPK or DAPKΔCaM on fibronectin-induced haptotaxis in MDA-MB-231 cells, which, again, could be rescued by TS2/16 (Fig. 8 D). These results indicate that DAPK is capable of inhibiting the migration of tumor cells that are resistant to the apoptotic effect of DAPK and suggest the existence of a second role for DAPK in tumor suppression.

Because the migratory capacity of tumor cells is one of the determining factors in their abilities to invade a matrix barrier, we tested the effect of DAPK on the invasiveness of the two tumor cells using Matrigel. As shown in Fig. 8 (E and F), the invasive potential of both cell lines was significantly reduced by overexpression of DAPK or DAPKΔCaM, and this effect was again reversed upon the addition of TS2/16. Furthermore, DAPK42A potentiated invasion of both A431 and MDA-MB-231 cells. In conclusion, our study identifies a novel function of DAPK in suppressing tumor cell migration and invasion, which is mediated by integrin inactivation but independent of apoptosis induction.

DAPK functions as a determining factor in tumor cell invasion

To further characterize the role of DAPK in tumor invasion, we used a pair of tumor cell lines. CL1-0 is a human lung adenocarcinoma cell line that was previously used to generate the highly invasive subline CL1-5 by progressive selections through the invasion chamber (Chu et al., 1997). We found that CL1-5 expressed a significantly lower level of DAPK than CL1-0 (Fig. 9 A), implying that reduction of DAPK expression conferred a selective advantage to develop a highly invasive phenotype during tumor progression. To determine whether DAPK expression level plays a role in the distinct invasiveness of the two cell lines, we overexpressed DAPK or DAPKΔCaM in CL1-5 cells (Fig. 9 B). As expected, such overexpression of DAPK or DAPKΔCaM led to a reduction in cell invasion, which was reversed by TS2/16 (Fig. 9 C). Next, we used DAPK siRNA to down-regulate the expression of endogenous DAPK in CL1-0 cells. DAPK level was significantly reduced in CL1-0 cells treated with DAPK-specific siRNA1 or siRNA2, but not with a control siRNA (Fig. 9 D). Compared with untransfected cells or cells receiving control siRNA, cells expressing either of the DAPK siRNAs displayed a marked increase in the invasion capability (Fig. 9 E). Together, these results not only demonstrate a role of endogenous DAPK in regulating tumor cell invasion, but also indicate that DAPK functions as one of the determining factors in the invasiveness of CL-1 cells.

Endogenous DAPK suppresses cell polarization during directed migration

We next investigated whether down-regulation of endogenous DAPK could affect cell polarization during migration. Using

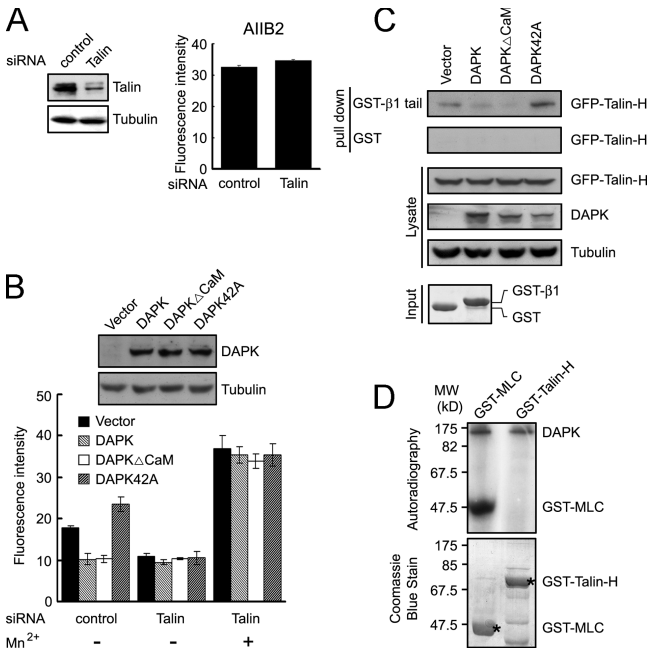

Figure 6. **DAPK interferes with talin-H binding to integrin.** (A) 293T cells were transfected with talin or control siRNA as indicated. Transfection efficiency was >90%. The expression of talin and tubulin were detected by Western blot (left), and the surface expression of integrin β1 was determined by flow cytometry analysis with antibody AIIB2 (right). (B) 293T cells cotransfected with talin or control siRNA and various DAPK constructs were treated with or without Mn^{2+} and then analyzed for cell surface binding of B44 (bottom). (top) The expression of various DAPK proteins. For the flow cytometry analyses in A and B, data shown are mean fluorescence intensities of B44 or AIIB2 binding subtracted by the background fluorescence intensities obtained from experiments using only the secondary antibody. $n = 3$. (C) 293T cells transfected with various forms of DAPK and GFP–talin-H were cultured in suspension and then lysed. Cell lysates were incubated with GST or GST-β1 tail, and GFP–talin-H bound on beads was analyzed by Western blot (top). The expression of various proteins in cell lysates was analyzed by Western blot (middle). (bottom) The equal input of GST and GST-β1 tail. (D) DAPK does not phosphorylate talin-H. Flag-tagged DAPK immunoprecipitated from lysate of transfected cells was used to phosphorylate bacterially expressed GST−myosin light chain (MLC) or GST–talin-H. Phosphorylated proteins were detected by autoradiography, and the positions of GST-MLC and autophosphorylated DAPK are indicated (top). The equal input of GST fusion proteins (*) is shown on the bottom.

a wound-scratch assay, we found that the parental CL1-0 cells or CL1-0 cells carrying control siRNA did not reorient their Golgi at 5 h after wounding (Fig. 9 F), and polarization began to emerge 7 h after wounding (not depicted). However, in cells receiving either of the DAPK-specific siRNAs, a significant population (~60%) sensed the wound and displayed Golgi reorientation at 5 h after wounding (Fig. 9, F and G). This finding identifies a physiological role of DAPK in the inhibition of cell polarization during directed migration.

Discussion

It is well documented that DAPK elicits proapoptotic activity. However, in this study, we uncover a novel biological function of DAPK in regulating cell migration. We found that DAPK inhibits random migration by suppressing directional persistence. During directed migration, DAPK functions as a potent inhibitor of cell polarization, as made evident by its perturbation of the formation of static protrusion at the leading edge, and polarization of MTOC and Golgi. Notably, these effects of DAPK are independent of its proapoptotic activity, as they are detected in cells without any sign of apoptosis. Indeed, even in cells that are resistant to DAPK-induced apoptosis, the migration/invasion inhibitory function of DAPK is still evident. We reason that this function of DAPK may contribute in part to its tumor-suppressive activity. In support of this notion, we found that the expression level of DAPK plays a determining role in the invasive capability of the CL1 cells, as increased expression of DAPK in CL1-5 cells inhibits tumor invasiveness, whereas decreased expression in CL1-0 cells promotes it. Notably, these alterations of DAPK expression in CL1-0 and CL1-5 cells did not significantly affect cell proliferation and survival (unpublished data), and therefore the role of DAPK in suppression of invasion is best explained by its motility effect.

The motility-inhibitory function of DAPK is expected to play two significant roles in suppressing tumor development and/or progression. First, as cell migration is central to tumor invasion through basement membrane and formation of metastasis in vivo, DAPK likely suppresses these processes through its effect on cell migration, thereby functioning in the late stage of tumor progression. Accordingly, DAPK has been demonstrated to suppress metastasis of Lewis lung carcinomas in a mouse model system (Inbal et al., 1997). Furthermore, hypermethylation of the DAPK gene and/or loss or reduction of DAPK expression have been shown to associate with metastasis and/or the advanced stages of many human cancer types (for reviews see Raveh and Kimchi, 2001; Bialik and Kimchi, 2004). Second, the motility-inhibitory effect of DAPK would be particularly important to suppress tumors that have escaped from DAPK-induced apoptosis, which can be achieved by mutations, leading to the inactivation of genes involved in the apoptosis core machinery, such as p53. Indeed, the apoptosis-promoting activity of DAPK is lost in many p53-defective tumor cell lines (Inbal et al., 2002; Wang et al., 2002), including the A431, MDA-MB-231, and CL1-5 cells used in this study. Given that inactivating mutations of p53 are frequently found in a wide range of human tumors, the migration/invasion inhibitory function of DAPK might be of greater clinical consequences than its proapoptotic role. Regardless of the relative contributions of the two mechanisms to tumor suppression, the proapoptotic and antimigratory activities of DAPK could act in a cooperative and complementary fashion to prevent malignancy during different stages of tumor development. This double safeguard mechanism would allow DAPK to act as an efficient and versatile tumor suppressor, which might explain the frequent observation of DAPK promoter hypermethylation in a wide variety of cancer types at different stages (for reviews see Raveh and Kimchi, 2001; Bialik and Kimchi, 2004). Importantly, both proapoptotic and antimigratory functions of DAPK are mainly medicated by integrin inactivation (Wang et al., 2002). Thus, integrin appears to play a central role in the tumor-suppressive effect of DAPK.

In this study, we not only demonstrate a critical role of integrin β1 in the motility-inhibitory function of DAPK but also explore the mechanism for DAPK-induced integrin inactivation.

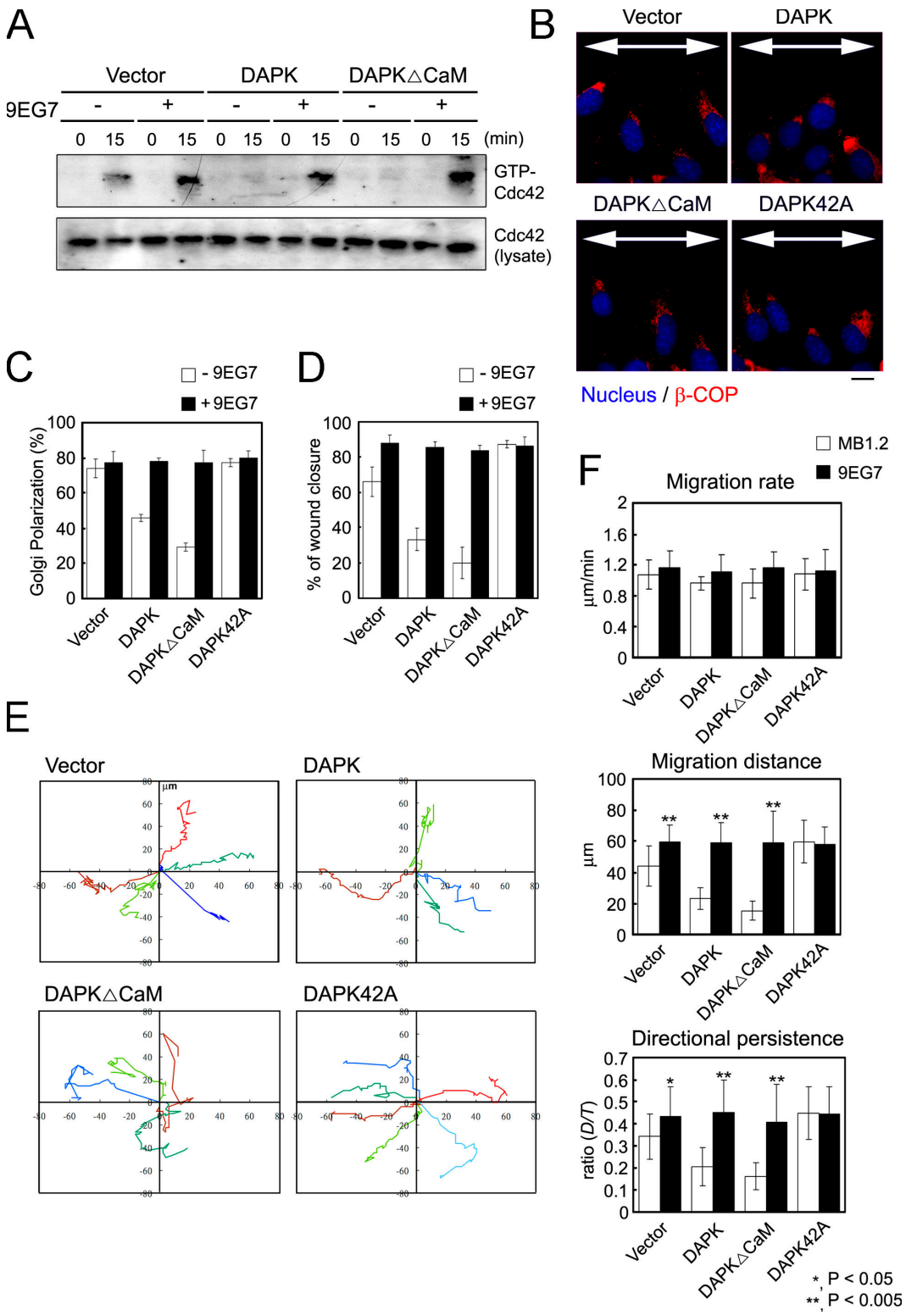

Figure 7. **Activation of integrin β1 rescues DAPK-induced migratory defects.** (A) A monolayer of NIH3T3 cells expressing various DAPK proteins was treated with or without 9EG7 before scratch. Cells were harvested 0 or 15 min after scratch and the amounts of GTP-bound and total Cdc42 were determined. (B) Cells as in A were analyzed for Golgi polarization 5 h after wounding. Arrows indicate the direction of the wound. (C) The percentage of cells, as in B, with polarized Golgi was quantitated. (D) A monolayer of NIH3T3 derivatives was treated with or without 9EG7 and assayed for wound-healing migration. The percentage of wound closure at 9 h after wounding was calculated. Data represent means ± SD. $n = 3$. (E) NIH3T3 cells expressing various DAPK proteins were treated with or without 9EG7 and assayed for random migration. The paths of representative cells during a 120-min period were plotted. (F) Cells, as in E, were assayed for free migration in the presence of 5 μg/ml 9EG7 or MB1.2 antibody. Migration parameters were calculated as in Fig. 1. Data represent means ± SD from trajectories of 30 cells. *, $P < 0.05$; **, $P < 0.005$, as compared with cells treated with MB1.2. Bar, 10 μm.

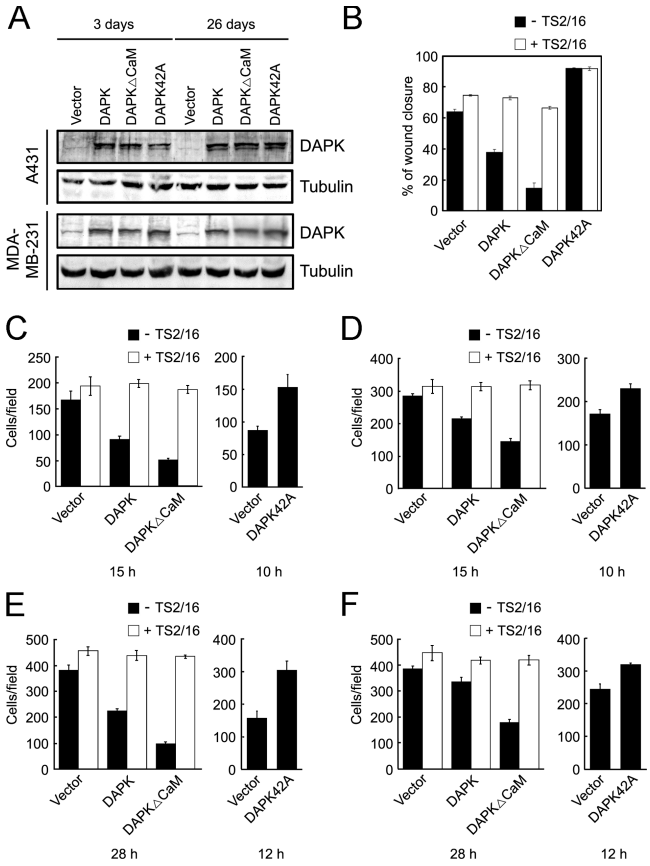

Figure 8. **DAPK inhibits migration and invasion in p53-defective tumor cell lines.** (A) A431 and MDA-MB-231 cells were infected with retrovirus-carrying vector or various forms of DAPK, selected by puromycin, left in culture for 3 or 26 d, and subjected to immunoblot analysis to detect the expression of DAPK proteins. (B) A431 cells were infected as in A, selected by puromycin for 3 d, and assayed for wound-healing migration in the presence or absence of TS2/16. The percentage of wound closure at 8 h after wounding was calculated. (C and D) The effect of DAPK on haptotactic migration. A431 (C) or MDA-MB-231 (D) cells expressing various DAPK proteins were assayed for haptotactic migration in the presence or absence of TS2/16. After the indicated time periods, cells that migrated to the lower side of the chamber were counted. (E and F) The effect of DAPK on invasion. A431 (E) or MDA-MB-231 (F) cells stably expressing various DAPK proteins were assayed for invasion through Matrigel. After the indicated time periods, cells invaded through Matrigel were counted. Data represent means ± SD. $n = 3$.

We first demonstrated that the integrin regulation function of DAPK or its mutants is completely abolished by depletion of talin, whereas activation of integrin by Mn^{2+} compensates for the effect of talin down-regulation. These results indicate that DAPK acts upstream of talin in regulating integrin activation. We further provide evidence showing that DAPK elicits an inhibitory effect on talin-H association with integrin β1 tail, a well known mechanism for inside-out activation of integrin (Calderwood et al., 2002, 2003; Garcia-Alvarez et al., 2003). As this inhibitory effect of DAPK can be detected in the absence of cell adhesion, it most likely represents a mechanism, rather than a consequence, of the integrin-modulating function of DAPK. How DAPK interferes with talin-H binding to integrin is currently unclear. However, the inability of DAPK to phosphorylate talin-H in vitro implies the involvement of an indirect mechanism. Additional studies are needed to elucidate whether DAPK signaling leads to an inhibitory posttranslational modification on talin-H or an activation of a competitor for talin-H–integrin interaction. Furthermore, as talin affects the activation status of multiple integrin β subunits (Tadokoro et al., 2003), it would be interesting to determine the effect of DAPK on the activities of other integrin β subunits.

Although the effects of DAPK on random and wound-healing migrations are described as the failure to maintain directional persistence and to establish cell polarity, respectively, these two events are likely to be mechanistically related. First, both events are rescued by enforced activation of integrin β1. Second, in both migration modes, DAPK- or DAPKΔCaM-expressing cells fail to establish a polarized morphology and static protrusion toward the direction of migration. In random migration, this leads to a decrease of directional persistence. In wound-healing migration, even though cells are unable to move toward different directions because of a lack of free space, this failure to maintain a polarized morphology would be expected to hamper efficient and persistent movement toward the wound, and therefore delays wound closure. Given that DAPK does not significantly alter migration speed in random migration, the effect of DAPK on wound-healing migration is predicted to be mainly resulted from the decrease of directional persistence.

The inability of DAPK to significantly reduce migration speed seems to be inconsistent with its integrin inactivation function, as cell-substratum adhesion strength plays a determining role in the migration speed of fibroblasts (Palecek et al., 1997). However, the actin cytoskeleton–localized DAPK might regulate other cytoskeleton-residing molecules to compensate for the effect of integrin inactivation on migration speed. Notably, DAPK was shown to phosphorylate myosin light chain at Ser19 in vivo, thereby increasing actomyosin contractility (Kuo et al., 2003). Future studies will be aimed at evaluating the contribution of this phosphorylation event to the migration properties of DAPK-expressing cells.

The effect of DAPK on migratory polarity and persistence is mainly attributed to its suppression of the integrin–Cdc42 polarity pathway. Although Cdc42 is well documented as a key polarity regulator (Etienne-Manneville, 2004), less attention has been focused on the role of integrin in controlling cell polarization. Inhibition of integrin function by a cyclic RGD peptide has been shown to block wound-induced Cdc42 activation and cell polarization in cultured astrocytes (Etienne-Manneville and Hall, 2001). This finding highlights a role of integrin in polarity establishment during directed migration, but the type of integrin involved in this process has not been defined. In this study, we identify integrin β1 as a crucial factor of polarity establishment during both random and directed migrations and as a mediator of DAPK-induced regulation of Cdc42 activity. Notably, a role of integrin β1 in polarized migration has been demonstrated in β1-null keratinocytes, which exhibit defects in the rapid reorientation of actin cytoskeletons toward the polarized movement (Raghavan et al., 2003). In addition, α4β1 integrin has been shown to regulate cell polarity during directed migration through its recruitment of the paxillin–GIT1 complex in the side and rear of cells to inhibit Rac activation (Nishiya et al., 2005). In contrast to these studies, a recent study demonstrated that

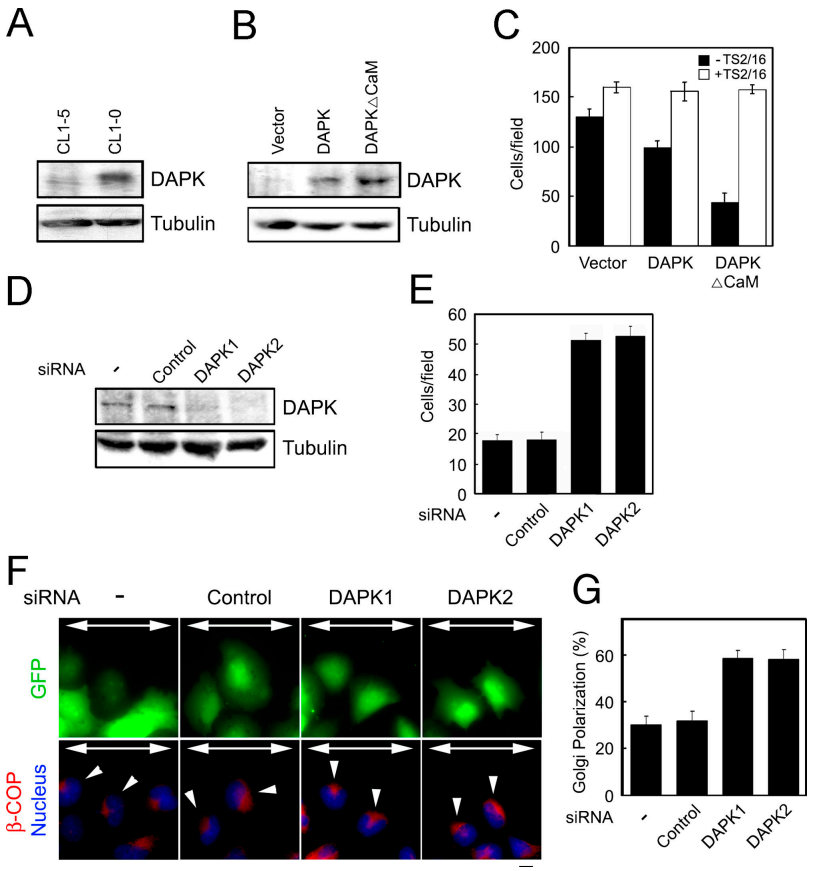

Figure 9. **DAPK level is a determining factor in tumor invasion.** (A) Analysis of DAPK expression in CL1-0 and CL1-5 cells by immunoblot analysis. (B) CL1-5 cells were transfected with DAPK or DAPKΔCaM and subjected to immunoblot analysis to detect the expression of DAPK proteins. (C) CL1-5 cells were transiently cotransfected with vector or various forms of DAPK, together with GFP, at a ratio of 4:1. Cells were treated with or without TS2/16 and assayed for their invasiveness. After 20 h of incubation, the GFP-positive cells invaded through Matrigel were counted. Data represent means ± SD. (D) CL1-0 cells were transiently transfected with control siRNA, DAPK siRNA1, or DAPK siRNA2, together with an expression vector for CD2-FAK. Transfected cells were isolated by the CELLetion CD2 kit, lysed, and subjected to immunoblot analysis to detect the expression of DAPK proteins. (E) CL1-0 cells were transfected with various siRNAs together with GFP at a ratio of 9:1. Transfected cells were assayed for their invasiveness, as in C, and the GFP-positive cells invaded through Matrigel were counted at 48 h after incubation. (F) A monolayer of CL1-0 cells transfected as in E was wounded. Cells were fixed 5 h after wounding and stained with anti–β-COP and Hoechst 33342. Arrows indicate the direction of the wound and small arrowheads mark the GFP-positive cells at the wound edge. (G) The percentage of GFP-positive cells as in F with polarized Golgi was measured in the front row cells. For each cell population, at least 150 cells were scored. Data represent means ± SD. $n = 3$. Bar, 10 μm.

adhesions mediated by αvβ3 are more static than those mediated by α β1. Consequently, αvβ3, rather than α5β1, permits the formation of a single broad lamellipod at the leading edge and persistent migration (Danen et al., 2005). Even though our study does not address the role of β3 in migration, we did observe the formation of static adhesion and persistent migration by activating β1 integrin in cells overexpressing DAPK or DAPKΔCaM. One explanation for this discrepancy in β1-mediated migration behavior may be the difference in migration speed of cells used in the two studies. As the GE11 epithelial cell used in a previous study (Danen et al.) migrates at a two- to threefold slower rate than the NIH3T3 fibroblast used in this study, more static cell-matrix adhesion (e.g., β3-mediated adhesion) may be needed to provide a sufficient time for the slow-migrating GE11 cells to complete the subsequent events in a migratory cycle. Alternatively, the downstream signaling events and migratory effect of β1 may be influenced by the existence of other types of integrin. Despite certain inconsistencies observed in different cell systems, these findings collectively underscore the importance of integrin-mediated cell-matrix adhesion in the establishment and/or maintenance of cell polarity during migration via its regulation of Rho family GTPases.

Materials and methods

Plasmids

pRK5- and pBabepuro-based expression vectors for DAPK, DAPKΔCaM, and DAPK42A were described previously (Jang et al., 2002; Wang et al., 2002). Human Cdc42V12 cDNA was obtained from T.-S. Jou (National Taiwan University, Taipei, Taiwan). The plasmid pGEX-β1 tail (residues 757–798 of the human integrin β1A cDNA) was obtained from H.-C. Chen (National Chung Hsing University, Taichung, Taiwan). The plasmid pGEX2T–talin-H (residues 1–435) was obtained from T.-L. Shen (National Taiwan University, Taipei, Taiwan), and the talin-H fragment was subcloned to pEGFPC1 vector.

Antibodies

The antibody to DAPK was described previously (Jang et al., 2002), and the human integrin β1-activating antibodies TS2/16 and AIIB2 were purified as described previously (Wang et al., 2002). The mouse β1 integrin–activating antibody 9EG7 was purchased from BD Biosciences, and the antibody to phosphorylated FAK (p-FAK) was purchased from Biosource International. The integrin β1 antibodies P4C10, B44, and MB1.2 were obtained from CHEMICON International, Inc. Antibodies to Cdc42 and Rap1 were purchased from Santa Cruz Biotechnology, Inc. Antibodies to β-COP and α-tubulin were obtained from Sigma-Aldrich. Antibody to γ-tubulin was obtained from S.-C. Lee (National Taiwan University, Taipei, Taiwan).

Cell culture, transfection, and retroviral infection

293T, NIH3T3, A431, and MDA-MB-231 cells were maintained as described previously (Wang et al., 2002; Chen et al., 2004). CL1-0 and CL1-5 cells (provided by P.-C. Yang, National Taiwan University, Taipei, Taiwan) were cultured in RPMI 1640 medium containing 10% FCS. Transfections of 293T, CL1-0, and CL1-5 cells were performed using the calcium phosphate method. Generation of recombinant retroviruses and infection of cells were performed following previously described procedures (Tsai et al., 2000).

Analysis of cell migration and invasion

For random migration analysis, cells were seeded on 6-well plates at a density of 10^4 cells/well in the regular culture medium and placed in a temperature- and CO_2-controlled chamber of a microscope (Axiovert 100TV; Carl Zeiss MicroImaging, Inc.) equipped with 20, 40, and 100× objective lenses. Time-lapse recording started 30 h after plating. Images were collected at 3-min intervals over 120 min with a cooled charge-coupled device (CCD) video camera (CollSNAP fx; Roper Scientific) operated by Metamorph image analysis software (Molecular Devices).

Motility parameters, including migration path, distance, rate, and directional persistence, were obtained from time-lapse movies. To track the migration path of individual cells, cells were manually traced for each frame and the geographical centers were recorded using Metamorph. The migration paths were expressed as graphs using the Excel program (Microsoft). The rates of cell migration were calculated as a ratio of the total length of migration paths and the duration of migration. Migration distances were determined as the net translocation during a 120-min period. Directional persistence was calculated as a ratio of the direct distance during a 120-min period and the total length of the migration path. For wound-healing migration assay, cells were seeded on 6-well plates at a density of 6×10^5 (for NIH3T3 cells) or 5×10^5 cells/well (for A431 cells) in culture medium. 30 h after seeding, the confluent monolayer of culture was scratched with a fine pipette tip, and migration was visualized by time-lapse imaging. The rate of wound closure was calculated by a ratio of the average distance between the two wound edges and the total duration of migration. For haptotactic migration assay, the underside of Transwell polycarbonate membrane (8-μm pore size; Costar) was coated with 15 ng/ml collagen I (for A431 cells) or 50 ng/ml fibronectin (for MDA-MB-231 cells). For the invasion assay, the membrane was coated with 0.54 μg/μl Matrigel (BD Biosciences). 10^5 cells resuspended in culture medium were plated onto the upper chamber, and the same medium was added to the lower chamber. Cells were incubated at 37°C for various time points. At the end point of incubation, cells on the upper side of the membrane were removed by wiping it with a cotton swab, and cells that had migrated onto the lower membrane surface were fixed by 4% formaldehyde, stained with Hoechst 33342, and counted. When transiently transfected cells were used, GFP-positive cells that had migrated to the underside of the membrane were counted under a fluorescence microscope (Axioskop; Carl Zeiss Microimaging, Inc.). Each assay was set up in triplicate, and ten random fields were analyzed for each membrane. To observe the effects of integrin β1 activation, 5 μg/ml 9EG7, 5 μg/ml MB1.2, or 2 μg/ml TS2/16 was added to culture medium before the recoding (for random and wound-healing migration) or to the upper chamber of Transwell plates.

Immunofluorescence analysis

Cells were fixed with 4% formaldehyde in PBS for 20 min. For β-COP staining, cells were permeabilized with PBS containing 0.01% Triton X-100 and 0.05% SDS for 5 min, and blocked with blocking solution (0.1% saponin and 0.2% BSA in PBS) for 30 min. Cells were incubated with β-COP antibody diluted in blocking solution for 2 h, and then incubated with Texas red–conjugated secondary antibody and Hoechst 33342 for 1 h. For integrin β1 (total or active), p-FAK, α-tubulin, or γ-tubulin staining, cells were permeabilized with extraction buffer containing 50 mM NaCl, 300 mM sucrose, 10 mM Pipes, pH 6.8, 3 mM $MgCl_2$, and 0.5% Triton X-100 for 5 min, blocked with PBS supplemented with 10% goat serum, 1% BSA, and 50 mM NH_4Cl for 1 h, and then incubated with various primary antibodies diluted in PBS containing 0.2% BSA and 5% goat serum for 1 h. Cells were then incubated with FITC- or Texas red–conjugated secondary antibody for 1 h. Cells were washed, mounted, and examined with either an epifluorescence microscope (Axioskop; Carl Zeiss MicroImaging, Inc.) with a 40 or 100× oil objective lens, or a confocal microscope (510 Meta; Carl Zeiss MicroImaging, Inc.) with a 100× oil objective lens. Fluorescent images were captured with a cooled CCD camera operated by the Image-Pro Plus Software (Media Cybernetics) or the Laser Scanning Microscope LSM510 Software. The images were arranged and labeled using Photoshop software (Adobe).

Cdc42 and Rap1 activity assays

Cdc42 (Kjoller and Hall, 2001) and Rap1 activity (Franke et al., 1997) were determined essentially as previously described. For Cdc42 activity, a monolayer of cells was repeatedly scratched (~30 times in a 60-mm dish) and lysed in a buffer containing 25 mM Hepes, pH 7.5, 150 mM NaCl, 1% Triton X-100, 10 mM $MgCl_2$, 1 mM EDTA, 10% glycerol, 1 mM PMSF, 10 μg/ml aprotinin, 10 μg/ml leupeptin, 1 mM sodium vanadate, 2 mM sodium pyrophosphate, and 10 mM NaF. For Rap1 activity, cells were lysed in lysis buffer containing 50 mM Tris, pH 7.4, 200 mM NaCl, 1% NP-40, 2.5 mM $MgCl_2$, 10% glycerol, 1 mM PMSF, 10 μg/ml aprotinin, and 10 μg/ml leupeptin. Cell lysates were incubated with GST-PAK-CRIB (for Cdc42) or GST-RalGDS-RBD (for Rap1; provided by J.L. Bos, University Medical Centre, Utrecht, Netherlands) coupled to glutathione–Sepharose 4B beads for 1 h at 4°C. The beads were washed, resuspended in SDS-PAGE sample buffer, and analyzed by Western blot with anti-Cdc42 antibody or anti-Rap1 antibody.

RNA interference

DAPK siRNAs, talin siRNAs (SMARTpool), and control siRNA were purchased from Dharmacon RNA Technologies. The sequences of DAPK siRNAs are as follows: DAPK siRNA1, sense: 5′-CAAGAAACGUUAGCAAAUGUU-3′ and antisense: 5′-CAUUUGCUAACGUUUCUUGUU-3′; DAPK siRNA2, sense: 5′-GGUCAAGGAUCCAAAGAAGUU-3′ and antisense: 5′-CUUCUUUGGAUCCUUGACCUU-3′. DAPK siRNAs were transfected to CL1-0 cells, together with a CD2 marker plasmid or a GFP plasmid. The transfected cells were isolated 48 h after transfection by CELLection CD2 kit (Dynal) or visualized by GFP fluorescence. Talin or control siRNA, together with various DAPK expression vectors, were cotransfected into 293T cells, and talin expression was determined at 72 h after transfection.

GST pull-down analysis

GST pull-down analysis was performed essentially as previously described (Chen et al., 2005). In brief, cells transiently cotransfected with GFP–talin-H and various DAPK constructs were cultured in suspension for 4 h and then lysed in lysis buffer containing 20 mM Tris, pH 8.0, 137 mM NaCl, 1% NP-40, 10% glycerol, 1 mM PMSF, 10 μg/ml aprotinin, 10 μg/ml leupeptin, 1 mM sodium vanadate, 2 mM sodium pyrophosphate, and 10 mM NaF. Lysate containing 2 mg of total proteins was incubated with 250 μg GST or GST–integrin β1 tail conjugated to glutathione beads, and bound protein was analyzed by Western blot.

Flow cytometry analysis

293T cells were cotransfected with various DAPK constructs and talin siRNA or control siRNA at a ratio of 1:1 and then treated with or without 5 mM $MnCl_2$ for 30 min. The total and active integrin β1 at cell surface were monitored by AIIB2 and B44 antibodies, respectively, followed by flow cytometry analysis as described previously (Wang et al., 2002).

In vitro kinase assay

To test protein phosphorylation by DAPK, Flag-tagged DAPK was immunoprecipitated from cell lysates and then incubated in 40 μl of kinase buffer containing 50 mM Hepes, pH 7.5, 8 mM $MgCl_2$, 2 mM $MnCl_2$, 0.1 mg/ml BSA, 1 μM bovine calmodulin (Sigma-Aldrich), 0.5 mM $CaCl_2$, 50 μM ATP, and 10 μCi γ-[^{32}P]ATP, in the presence 2 μg GST-MLC or GST–talin-H at 25°C for 15 min. Protein phosphorylation was detected by autoradiography.

Online supplemental material

The effect of DAPK on Rap1 activity, random and wound-healing migrations of 9EG7-treated cells, as well as the cell death and wound-healing migration assays for A431 stable transfectants are provided as supplemental figures. In addition, supplemental videos of migratory experiments are provided. Online supplemental material is available at http://www.jcb.org/cgi/content/full/jcb.200505138/DC1.

We thank the Microarray Core Facility for Genomic Medicine of the National Research Program for Genomic Medicine and the National Taiwan University Center of Genomic medicine for the time-lapse microscope.

This work was supported by National Science Council Frontier grant NSC94-2321-B-002-013, Academia Sinica Thematic Project AS-95-TP-B02, and National Taiwan University Hospital research grant NTUH 93-5052.

Submitted: 23 May 2005
Accepted: 12 January 2006

References

Allen, W.E., D. Zicha, A.J. Ridley, and G.E. Jones. 1998. A role for Cdc42 in macrophage chemotaxis. *J. Cell Biol.* 141:1147–1157.

Bialik, S., and A. Kimchi. 2004. DAP-kinase as a target for drug design in cancer and diseases associated with accelerated cell death. *Semin. Cancer Biol.* 14:283–294.

Bialik, S., A.R. Bresnick, and A. Kimchi. 2004. DAP-kinase-mediated morphological changes are localization dependent and involve myosin-II phosphorylation. *Cell Death Differ.* 11:631–644.

Calderwood, D.A., B. Yan, J.M. de Pereda, B.G. Alvarez, Y. Fujioka, R.C. Liddington, and M.H. Ginsberg. 2002. The phosphotyrosine binding-like domain of talin activates integrins. *J. Biol. Chem.* 277:21749–21758.

Calderwood, D.A., Y. Fujioka, J.M. de Pereda, B. Garcia-Alvarez, T. Nakamoto, B. Margolis, C.J. McGlade, R.C. Liddington, and M.H. Ginsberg. 2003. Integrin beta cytoplasmic domain interactions with phosphotyrosine-binding domains: a structural prototype for diversity in integrin signaling. *Proc. Natl. Acad. Sci. USA*. 100:2272–2277.

Cau, J., and A. Hall. 2005. Cdc42 controls the polarity of the actin and microtubule cytoskeletons through two distinct signal transduction pathways. *J. Cell Sci.* 118:2579–2587.

Chen, C.H., W.J. Wang, J.C. Kuo, H.C. Tsai, J.R. Lin, Z.F. Chang, and R.H. Chen. 2005. Bidirectional signals transduced by DAPK-ERK interaction promote the apoptotic effect of DAPK. *EMBO J.* 24:294–304.

Chen, H.Y., C.H. Shen, Y.T. Tsai, F.C. Lin, Y.P. Huang, and R.H. Chen. 2004. Brk activates rac1 and promotes cell migration and invasion by phosphorylating paxillin. *Mol. Cell. Biol.* 24:10558–10572.

Chu, Y.W., P.C. Yang, S.C. Yang, Y.C. Shyu, M.J. Hendrix, R. Wu, and C.W. Wu. 1997. Selection of invasive and metastatic subpopulations from a human lung adenocarcinoma cell line. *Am. J. Respir. Cell Mol. Biol.* 17:353–360.

Cohen, O., E. Feinstein, and A. Kimchi. 1997. DAP-kinase is a Ca^{2+}/calmodulin-dependent, cytoskeletal-associated protein kinase, with cell death-inducing functions that depend on its catalytic activity. *EMBO J.* 16:998–1008.

Cohen, O., B. Inbal, J.L. Kissil, T. Raveh, H. Berissi, T. Spivak-Kroizaman, E. Feinstein, and A. Kimchi. 1999. DAP-kinase participates in TNF-α–and Fas-induced apoptosis and its function requires the death domain. *J. Cell Biol.* 146:141–148.

Cox, E.A., S.K. Sastry, and A. Huttenlocher. 2001. Integrin-mediated adhesion regulates cell polarity and membrane protrusion through the Rho family of GTPases. *Mol. Biol. Cell*. 12:265–277.

Danen, E.H., J. van Rheenen, W. Franken, S. Huveneers, P. Sonneveld, K. Jalink, and A. Sonnenberg. 2005. Integrins control motile strategy through a Rho–cofilin pathway. *J. Cell Biol.* 169:515–526.

Deiss, L.P., E. Feinstein, H. Berissi, O. Cohen, and A. Kimchi. 1995. Identification of a novel serine/threonine kinase and a novel 15-kD protein as potential mediators of the gamma interferon-induced cell death. *Genes Dev.* 9:15–30.

Etienne-Manneville, S. 2004. Cdc42–the centre of polarity. *J. Cell Sci.* 117:1291–1300.

Etienne-Manneville, S., and A. Hall. 2001. Integrin-mediated activation of Cdc42 controls cell polarity in migrating astrocytes through PKCzeta. *Cell*. 106:489–498.

Etienne-Manneville, S., and A. Hall. 2003. Cdc42 regulates GSK-3beta and adenomatous polyposis coli to control cell polarity. *Nature*. 421:753–756.

Franke, B., J.N. Akkerman, and J.L. Bos. 1997. Rapid Ca^{2+}-mediated activation of Rap1 in human platelets. *EMBO J.* 16:252–259.

Fukata, M., T. Watanabe, J. Noritake, M. Nakagawa, M. Yamaga, S. Kuroda, Y. Matsuura, A. Iwamatsu, F. Perez, and K. Kaibuchi. 2002. Rac1 and Cdc42 capture microtubules through IQGAP1 and CLIP-170. *Cell*. 109:873–885.

Garcia-Alvarez, B., J.M. de Pereda, D.A. Calderwood, T.S. Ulmer, D. Critchley, I.D. Campbell, M.H. Ginsberg, and R.C. Liddington. 2003. Structural determinants of integrin recognition by talin. *Mol. Cell*. 11:49–58.

Im, E.O., Y.H. Choi, K.J. Paik, H. Suh, Y. Jin, K.W. Kim, Y.H. Yoo, and N.D. Kim. 2001. Novel bile acid derivatives induce apoptosis via a p53-independent pathway in human breast carcinoma cells. *Cancer Lett.* 163:83–93.

Inbal, B., O. Cohen, S. Polak-Charcon, J. Kopolovic, E. Vadai, L. Eisenbach, and A. Kimchi. 1997. DAP kinase links the control of apoptosis to metastasis. *Nature*. 390:180–184.

Inbal, B., S. Bialik, I. Sabanay, G. Shani, and A. Kimchi. 2002. DAP kinase and DRP-1 mediate membrane blebbing and the formation of autophagic vesicles during programmed cell death. *J. Cell Biol.* 157:455–468.

Itoh, R.E., K. Kurokawa, Y. Ohba, H. Yoshizaki, N. Mochizuki, and M. Matsuda. 2002. Activation of rac and cdc42 video imaged by fluorescent resonance energy transfer-based single-molecule probes in the membrane of living cells. *Mol. Cell. Biol.* 22:6582–6591.

Jang, C.W., C.H. Chen, C.C. Chen, J.Y. Chen, Y.H. Su, and R.H. Chen. 2002. TGF-beta induces apoptosis through Smad-mediated expression of DAP-kinase. *Nat. Cell Biol.* 4:51–58.

Kinbara, K., L.E. Goldfinger, M. Hansen, F.-L. Chou, and M.H. Ginsberg. 2003. Ras GTPases: integrins' friends or foes? *Nat. Rev. Mol. Cell Biol.* 4:767–776.

Kjoller, L., and A. Hall. 2001. Rac mediates cytoskeletal rearrangements and increased cell motility induced by urokinase-type plasminogen activator receptor binding to vitronectin. *J. Cell Biol.* 152:1145–1157.

Kuo, J.-C., J.-R. Lin, J.M. Staddon, H. Hosoya, and R.-H. Chen. 2003. Uncoordinated regulation of stress fibers and focal adhesions by DAP-kinase. *J. Cell Sci.* 116:4777–4790.

Lauffenburger, D.A., and A.F. Horwitz. 1996. Cell migration: a physically integrated molecular process. *Cell*. 84:359–369.

Logunov, D.Y., G.V. Ilyinskaya, L.V. Cherenova, L.V. Verhovskaya, M.M. Shmarov, P.M. Chumakov, B.P. Kopnin, and B.S. Naroditsky. 2004. Restoration of p53 tumor-suppressor activity in human tumor cells in vitro and in their xenografts in vivo by recombinant avian adenovirus CELO-p53. *Gene Ther.* 11:79–84.

Ni, H., A. Li, N. Simonsen, and J.A. Wilkins. 1998. Integrin activation by dithiothreitol or Mn^{2+} induces a ligand-occupied conformation and exposure of a novel NH_2-terminal regulatory site on the β1 integrin chain. *J. Biol. Chem.* 273:7981–7987.

Nishiya, N., W.B. Kiosses, J. Han, and M.H. Ginsberg. 2005. An alpha(4) integrin-paxillin-Arf-GAP complex restricts Rac activation to the leading edge of migrating cells. *Nat. Cell Biol.* 7:343–352.

Nobes, C.D., and A. Hall. 1999. Rho GTPases control polarity, protrusion, and adhesion during cell movement. *J. Cell Biol.* 144:1235–1244.

Palecek, S.P., J.C. Loftus, M.H. Ginsberg, D.A. Lauffenburger, and A.F. Horwitz. 1997. Integrin-ligand binding properties govern cell migration speed through cell-substratum adhesiveness. *Nature*. 385:537–540.

Pelled, D., T. Raveh, C. Riebeling, M. Fridkin, H. Berissi, A.H. Futerman, and A. Kimchi. 2002. Death-associated protein (DAP) kinase plays a central role in ceramide-induced apoptosis in cultured hippocampal neurons. *J. Biol. Chem.* 277:1957–1961.

Raftopoulou, M., and A. Hall. 2004. Cell migration: Rho GTPases lead the way. *Dev. Biol.* 265:23–32.

Raghavan, S., A. Vaezi, and E. Fuchs. 2003. A role for alphabeta1 integrins in focal adhesion function and polarized cytoskeletal dynamics. *Dev. Cell*. 5:415–427.

Raveh, T., and A. Kimchi. 2001. DAP kinase-a proapoptotic gene that functions as a tumor suppressor. *Exp. Cell Res.* 264:185–192.

Raveh, T., G. Droguett, M.S. Horwitz, R.A. DePinho, and A. Kimchi. 2001. DAP kinase activates a p19ARF/p53-mediated apoptotic checkpoint to suppress oncogenic transformation. *Nat. Cell Biol.* 3:1–7.

Ridley, A.J., M.A. Schwartz, K. Burridge, R.A. Firtel, M.H. Ginsberg, G. Borisy, J.T. Parsons, and A.R. Horwitz. 2003. Cell migration: integrating signals from front to back. *Science*. 302:1704–1709.

Stramer, B., W. Wood, M.J. Galko, M.J. Redd, A. Jacinto, S.M. Parkhurst, and P. Martin. 2005. Live imaging of wound inflammation in *Drosophila* embryos reveals key roles for small GTPases during in vivo cell migration. *J. Cell Biol.* 168:567–573.

Tadokoro, S., S.J. Shattil, K. Eto, V. Tai, R.C. Liddington, J.M. de Pereda, M.H. Ginsberg, and D.A. Calderwood. 2003. Talin binding to integrin beta tails: a final common step in integrin activation. *Science*. 302:103–106.

Tsai, Y.T., Y.H. Su, S.S. Fang, T.N. Huang, Y. Qiu, Y.S. Jou, H.M. Shih, H.J. Kung, and R.H. Chen. 2000. Etk, a Btk family tyrosine kinase, mediates cellular transformation by linking Src to STAT3 activation. *Mol. Cell. Biol.* 20:2043–2054.

Wang, W.J., J.C. Kuo, C.C. Yao, and R.H. Chen. 2002. DAP-kinase induces apoptosis by suppressing integrin activity and disrupting matrix survival signals. *J. Cell Biol.* 159:169–179.

Watanabe, T., S. Wang, J. Noritake, K. Sato, M. Fukata, M. Takefuji, M. Nakagawa, N. Izumi, T. Akiyama, and K. Kaibuchi. 2004. Interaction with IQGAP1 links APC to Rac1, Cdc42, and actin filaments during cell polarization and migration. *Dev. Cell*. 7:871–883.

Yamamoto, M., T. Hioki, T. Ishii, S. Nakajima-Iijima, and S. Uchino. 2002. DAP kinase activity is critical for C(2)-ceramide-induced apoptosis in PC12 cells. *Eur. J. Biochem.* 269:139–147.